



ISSN NO. 2320-5407

Journal homepage: <http://www.journalijar.com>

INTERNATIONAL JOURNAL
OF ADVANCED RESEARCH

RESEARCH ARTICLE

Effects of Adhesive and Interphase Characteristics between Matrix and Reinforced Nanoparticle of AA5154/AlN Nanocomposites

A. Chennakesava Reddy

Department of Mechanical Engineering, JNTUH College of Engineering, Hyderabad, India,

Manuscript Info

Manuscript History:

Received: 15 July 2015

Final Accepted: 22 August 2015

Published Online: September 2015

Key words:

RVE models, AlN, AA5154, finite element analysis, interphase

*Corresponding Author

A. Chennakesava Reddy

Abstract

The interphase is formed due to chemical reaction between the matrix and filler materials or the use of protective coatings on the reinforcement during manufacturing. It is the weakest link in the load path, and consequently most failures in particulate reinforced composites, such as debonding, and matrix cracking, occur in or near this region. In this article two types of RVE models have been implemented using finite element analysis. Aluminum nitride nanoparticles were used as a reinforcing material in the matrix of AA5154 aluminum alloy. It has been observed that the nanoparticle did not overload during the transfer of load from the matrix to the nanoparticle via the interphase due to existence of interphase between the nanoparticle and the matrix. The tensile strength has increased from 424.22 to 435.78 MPa with an interphase around aluminum nitride nanoparticle in the AA5154/AlN nanocomposites.

Copy Right, IJAR, 2015.. All rights reserved

INTRODUCTION

Metal matrix composites (MMCs) have been drawn attention in recent years owing to the need for materials with high strength and stiffness in the field for a large number of functional and structural applications. The higher stiffness of ceramic particles can lead to an incremental increase in the stiffness of a composite (Reddy, 2009; Reddy & Zitoun, 2011). One of the major challenges when processing nanocomposites is achieving a homogeneous distribution of reinforcement in the matrix as it has a strong impact on the properties and the quality of the material. The current processing methods often generate agglomerated particles in the ductile matrix and as a result they exhibit extremely low ductility (Deng & Chawla, 2006). Particle clusters act as crack or decohesion nucleation sites at stresses lower than the matrix yield strength, causing the nanocomposite to fail at unpredictable low stress levels. Possible reasons resulting in particle clustering are chemical binding, surface energy reduction or particle segregation (Reeves et al., 1992; Kotiveerachari & Reddy, 1999; Reddy, 2004)]. While manufacturing Al alloy-AlN nanocomposites, the wettability factor is the main concern irrespective of the manufacturing method. Its high surface activity restricts its incorporation in the metal matrix. One of the methods is to add surfactant which acts as a wetting agent in molten metal to enhance wettability of particulates. Researchers have successfully used several surfactants like Li, Mg, Ca, Zr, Ti, Cu, and Si for the synthesis of nanocomposites (Ren, 2011; Sobczak et al., 1993; Davidson & Regenar, 2000).

The objective of this article was to develop AA5154/AlN nanocomposites with and without wetting criteria of AlN by AA5154 molten metal. The RVE models were used to analyze the nanocomposites using finite Element analysis. A homogeneous interphase region was assumed in the models.

1. Theoretical Background

Analyzing structures on a microstructural level, however, is clearly an inflexible problem. Analysis methods have therefore sought to approximate composite structural mechanics by analyzing a representative section of the composite microstructure, commonly called a Representative Volume Element (RVE). One of the first formal

definitions of the RVE was given by Hill, 1963 who stated that the RVE was (1) structurally entirely typical of the composite material on average and (2) contained a sufficient number of inclusions such that the apparent moduli were independent of the RVE boundary displacements or tractions. Under axisymmetric as well as antisymmetric loading, a 2-D axisymmetric model can be applied for the cylindrical RVE, which can significantly reduce the computational work (Liu & Chen, 2003).

2.1 Determination Effective Material Properties

To derive the formulae for deriving the equivalent material constants, a homogenized elasticity model of the square representative volume element (RVE) as shown in figure 1 is considered. The dimensions of the three-dimensional RVE are $2a \times 2a \times 2a$. The cross-sectional area of the RVE is $2a \times 2a$. The elasticity model is filled with a single, transversely isotropic material that has five independent material constants (elastic moduli E_y and E_z , Poisson’s ratios ν_{xy} , ν_{yz} and shear modulus G_{yz}). The general strain-stress relations relating the normal stresses and the normal strains are given below:

$$\epsilon_x = \frac{\sigma_x}{E_x} - \frac{\nu_{xy} \sigma_y}{E_y} - \frac{\nu_{xz} \sigma_z}{E_z} \tag{1}$$

$$\epsilon_y = -\frac{\nu_{yx} \sigma_x}{E_y} + \frac{\sigma_y}{E_y} - \frac{\nu_{yz} \sigma_z}{E_z} \tag{2}$$

$$\epsilon_z = -\frac{\nu_{zx} \sigma_x}{E_x} - \frac{\nu_{zy} \sigma_y}{E_y} + \frac{\sigma_z}{E_z} \tag{3}$$

Let assume that $\sigma_{xy} = \sigma_{yx}$, $\sigma_{yz} = \sigma_{zy}$ and $\sigma_{zx} = \sigma_{xz}$. For plane strain conditions, $\epsilon_z = 0$, $\epsilon_{yz} = \epsilon_{zx} = 0$ and $\epsilon_{yz} = \epsilon_{zx}$. The above equations are rewritten as follows:

$$\epsilon_x = \frac{\sigma_x}{E_x} - \frac{\nu_{xy} \sigma_y}{E_y} - \frac{\nu_{yz} \sigma_z}{E_z} \tag{4}$$

$$\epsilon_y = -\frac{\nu_{xy} \sigma_x}{E_y} + \frac{\sigma_y}{E_y} - \frac{\nu_{yz} \sigma_z}{E_z} \tag{5}$$

$$\epsilon_z = -\frac{\nu_{yz} \sigma_x}{E_z} - \frac{\nu_{yz} \sigma_y}{E_z} + \frac{\sigma_z}{E_z} \tag{6}$$

To determine E_y and E_z , ν_{xy} and ν_{yz} , four equations are required. Two loading cases as shown in figure 2 have been designed to give four such equations based on the theory of elasticity. For load case (figure 2a), the stress and strain components on the lateral surface are:

$$\begin{aligned} \sigma_x &= \sigma_y = 0 \\ \epsilon_x &= \frac{\Delta a}{a} \text{ along } x = \pm a \text{ and } \epsilon_y = \frac{\Delta a}{a} \text{ along } y = \pm a \\ \epsilon_z &= \frac{\Delta a}{a} \end{aligned}$$

where Δa is the change of dimension a of cross-section under the stretch Δa in the z -direction. Integrating and averaging Eq. (6) on the plane $z = a$, the following equation can be arrived:

$$E_z = \frac{\sigma_{ave}}{\epsilon_z} = \frac{a}{\Delta a} \sigma_{ave} \tag{7}$$

where the average value of σ_z is given by:

$$\sigma_{ave} = \iint \sigma_z(x, y, a) dx dy \tag{8}$$

The value of σ_{ave} is evaluated for the RVE using finite element analysis (FEA) results.

Using Eq. (5) and the result (7), the strain along $y = \pm a$:

$$\epsilon_y = -\frac{\nu_{yz} \sigma_z}{E_z} = -\nu_{yz} \frac{\Delta a}{a} = \frac{\Delta a}{a}$$

Hence, the expression for the Poisson’s ratio ν_{yz} is as follows:

$$\nu_{yz} = -1 \tag{9}$$

For load case (figure 2b), the square representative volume element (RVE) is loaded with a uniformly distributed load (negative pressure), P in a lateral direction, for instance, the x -direction. The RVE is constrained in the z -direction so that the plane strain condition is sustained to simulate the interactions of RVE with surrounding materials in the z -direction. Since $\epsilon_z = 0$, $\sigma_z = \nu_{yz}(\sigma_x + \sigma_y)$ for the plain stress, the strain-stress relations can be reduced as follows:

$$\epsilon_x = \left(\frac{1}{E_x} - \frac{1}{E_z}\right) \sigma_x - \left(\frac{\nu_{xy}}{E_y} + \frac{1}{E_z}\right) \sigma_y \tag{10}$$

$$\epsilon_y = -\left(\frac{\nu_{xy}}{E_x} + \frac{1}{E_z}\right) \sigma_x + \left(\frac{1}{E_x} - \frac{1}{E_z}\right) \sigma_y \tag{11}$$

For the elasticity model as shown in figure 2b, one can have the following results for the normal stress and strain components at a point on the lateral surface:

$$\sigma_y = 0, \sigma_x = P$$

$$\varepsilon_x = \frac{\Delta x}{a} \text{ along } x = \pm a \text{ and } \varepsilon_y = \frac{\Delta y}{a} \text{ along } y = \pm a$$

where $\Delta x (>0)$ and $\Delta y (<0)$ are the changes of dimensions in the x- and y- direction, respectively for the load case shown in figure 2b. Applying Eq. (11) for points along $y = \pm a$ and Eq. (10) for points along $x = \pm a$, we get the following:

$$\varepsilon_y = -\left(\frac{v_{xy}}{E_x} + \frac{1}{E_z}\right)P = \frac{\Delta y}{a} \quad (12)$$

$$\varepsilon_x = \left(\frac{1}{E_x} - \frac{1}{E_z}\right)P = \frac{\Delta x}{a} \quad (13)$$

By solving Eqs. (12) and (13), the effective elastic modulus and Poisson's ratio in the transverse direction (xy-plane) as follows:

$$E_x = E_y = \frac{1}{\frac{\Delta x}{Pa} + \frac{1}{E_z}} \quad (14)$$

$$v_{xy} = \left(\frac{\Delta y}{Pa} + \frac{1}{E_z}\right) / \left(\frac{\Delta x}{Pa} + \frac{1}{E_z}\right) \quad (15)$$

In which E_z can be determined from Eq. (7). Once the change in lengths along x- and y- direction (Δx and Δy) are determined for the square RVE from the FEA, $E_y (= E_x)$ and v_{xy} can be determined from Eqs. (14) and (15), correspondingly.

2.2 Empirical Models for Elastic Moduli and Strength of Nanocomposites

The strength of a particulate metal matrix composite depends on the strength of the weakest zone and metallurgical phenomena in it (Reddy, 2015). A new criterion is suggested by the author considering adhesion, formation of precipitates, particle size, agglomeration, voids/porosity, obstacles to the dislocation, and the interfacial reaction of the particle/matrix. The formula for the strength of composite is stated below:

$$\sigma_c = \left[\sigma_m \left\{ \frac{1-(v_p+v_v)^{2/3}}{1-1.5(v_p+v_v)} \right\} \right] e^{m_p(v_p+v_v)} + k d_p^{-1/2} \quad (16)$$

$$k = E_m m_m / E_p m_p$$

where, v_v and v_p are the volume fractions of voids/porosity and nanoparticles in the composite respectively, m_p and m_m are the poisson's ratios of the nanoparticles and matrix respectively, d_p is the mean nanoparticle size (diameter) and E_m and E_p is elastic moduli of the matrix and the particle respectively. Elastic modulus (Young's modulus) is a measure of the stiffness of a material and is a quantity used to characterize materials. Elastic modulus is the same in all orientations for isotropic materials. Anisotropy can be seen in many composites. The proposed equations (Reddy, 2015) by the author to find Young's modulus of composites and interphase including the effect of voids/porosity as given below:

The upper-bound equation is given by

$$\frac{E_c}{E_m} = \left(\frac{1-v_v^{2/3}}{1-v_v^{2/3}+v_v} \right) + \frac{1+(\delta-1)v_p^{2/3}}{1+(\delta-1)(v_p^{2/3}-v_p)} \quad (17)$$

The lower-bound equation is given by

$$\frac{E_c}{E_m} = 1 + \frac{v_p-v_v}{\delta/(\delta-1)-(v_p+v_v)^{1/3}} \quad (18)$$

where, $\delta = E_p/E_m$.

The transverse modulus is given by

$$E_t = \frac{E_m E_p}{E_m + E_p(1-v_p^{2/3})/v_p^{2/3}} + E_m(1 - v_p^{2/3} - v_v^{2/3}) \quad (19)$$

The young's modulus of the interphase is obtained by the following formula:

$$E_i(r) = (\alpha E_p - E_m) \left(\frac{r_i-r}{r_i-r_p} \right) + E_m \quad (20)$$

2. Materials Methods

The matrix material was AA5154 aluminum alloy. AA5154 contains Si (12.50%), Cr ($\leq 0.10\%$), Cu (1.20%), Fe ($\leq 1.00\%$), Mg (1.10%), Ni (1.00%) and Zn ($\leq 0.25\%$) as its major alloying elements. The reinforcement material was aluminum nitride (AlN) nanoparticles of average size 100nm. The mechanical properties of materials used in the present work are given in table 1.

The representative volume element (RVE or the unit cell) is the smallest volume over which a measurement can be made that will yield a value representative of the whole. In this research, a cubical RVE was implemented to analyze the tensile behavior AA3015/AlN nanocomposites (figure 6). The determination of the

RVE's dimensional conditions requires the establishment of a volumetric fraction of spherical nanoparticles in the composite. Hence, the weight fractions of the particles were converted to volume fractions. The volume fraction of a particle in the RVE ($V_{p,rve}$) is determined using Eq.(21):

$$v_{p,rve} = \frac{\text{Volume of nanoparticle}}{\text{Volume of RVE}} = \frac{16}{3} \times \left(\frac{r}{a}\right)^3 \quad (21)$$

where, r represents the particle radius and a indicates the diameter of the cylindrical RVE. The volume fraction of the particles in the composite (V_p) is obtained using equation

$$V_p = (w_p/\rho_p)/(w_p/\rho_p + w_m/\rho_m) \quad (22)$$

where ρ_m and ρ_p denote the matrix and particle densities, and w_m and w_p indicate the matrix and particle weight fractions, respectively.

The RVE dimension (a) was determined by equalizing Eqs. (21) and (22). Two RVE schemes namely: without interphase (adhesion) and with interphase were applied between the matrix and the filler. The loading on the RVE was defined as symmetric displacement, which provided equal displacements at both ends of the RVE. To obtain the nanocomposite modulus and yield strength, the force reaction was defined against displacement. The large strain PLANE183 element (Alavala, 2008) was used in the matrix and the interphase regions in all the models. In order to model the adhesion between the interphase and the particle, a COMBIN14 spring-damper element was used. The stiffness of this element was taken as unity for perfect adhesion which could determine the interfacial strength for the interface region.

To converge an exact nonlinear solution, it is also important to set the strain rates of the FEM models based on the experimental tensile tests' setups. Hence, FEM models of different RVEs with various particle contents should have comparable error values. In this respect, the ratio of the tensile test speed to the gauge length of the specimens should be equal to the corresponding ratio in the RVE displacement model. Therefore, the rate of displacement in the RVEs was set to be 0.1 (1/min).

3. Result and Discussion

The AlN/AA5154 nanocomposites with or without interphase were modeled using finite element analysis (ANSYS) to analyze the tensile behavior and fracture.

4.1 Tensile Behavior

An increase of AlN content in the matrix could increase the tensile strength of the nanocomposite (figure 3). The maximum difference between the FEA results without interphase and the experimental results was 54.95 MPa. This differentiation can be attributed to lack of bonding between the AlN nanoparticle and the AA5154 matrix. The maximum difference between the FEA results with interphase and the experiments results was 43.55 MPa. This discrepancy can be endorsed to the presence of voids in the nanocomposites. Author's model includes the effect of voids present in the nanocomposite. The results obtained from author's model (with voids) were nearly equal to the experimental values with maximum variation of 24.29 MPa. On the other hand, the deviation of FEA (RVE model) results with the experimental results possibly was as a result of micro-metallurgical factors (such as formation of voids and nanoparticle clustering) that were not considered in the RVE models.

For 10%, 20% and 30% V_p of AlN in AA5154, without interphase and barely consideration of adhesive bonding between the AlN nanoparticle and the AA5154 matrix, the loads transferred from the AlN nanoparticle to the AA5154 matrix were, respectively, 65.08 MPa, 102.36 MPa and 104.29 MPa (figure 4) along the tensile load direction. Similarly, for 10%, 20% and 30% V_p of AlN in AA5154, with interphase and wetting between the ALN nanoparticle and the AA5154 matrix, the loads transferred from the AlN nanoparticle to the AA5154 matrix were, respectively, 97.90 MPa, 134.42 MPa and 108.31 MPa (figure 4) along the tensile load direction. Zhengang et al (Zhengang et al., 2010) carried a study improving wettability by adding Mg as the wetting agent. They suggested that the wettability between molten Al-Mg matrix and SiC particles is improved and the surface tension of molten Al-Mg alloy with SiC particle is reduced, and results in homogeneous particles distribution and high interfacial bond strength. For instance, addition of Mg to composite matrix lead to the formation of MgO and $MgAl_2O_3$ at the interface and this enhances the wettability and the strength of the composite (Reddy & Zitoun, 2009).

According to strains developed in the nanocomposites (figure 5), the RVE was expanded elastically away from the particle in the direction of the tensile loading. This would increase the contact area between the particle and the matrix in the perpendicular direction to the tensile loading and would decrease the contact area between the particle and the matrix in the direction of the tensile loading. In addition, the deformation was propagated from the matrix to the nanoparticle in the normal direction to the tensile loading. The same kind of trend was observed with the nanocomposites consisting of interphase. The only difference was the propagation of deformation from the

matrix to the nanoparticle. This was high with interphase as it would improve the wettability of the nanoparticle with the matrix. The interphase extends the yielding character of the nano composite. For the homogenization analysis only one cell was analyzed for each volume fraction since the periodicity assumption gives the same result for any number of cells. The local RVE strain was not equal to the average RVE strain but fluctuates about the average RVE strain. The relationship between the average RVE strain and any applied boundary condition was not unique. Increasing the nanoparticle volume fraction reduce the effect of boundary conditions on the variation of the RVE local strain distribution.

By increasing the volume fraction of AlN, the tensile elastic modulus increased appreciably (figure 6). The results of tensile moduli obtained FEA were within the limits of author's models and were closer to the results obtained by the Rule of Mixture. The transverse moduli were nearly equal to the results obtained by the author's models and the Rule of Mixture.

4.2 Fracture

Figure 7 depicts the increase of von Mises stress with increase of volume fraction of AlN. The shear stresses induced in the nanocomposites with and without interphase are shown in figure 8. In the case of nanocomposites with interphase between the nanoparticle and the matrix, the stress was transferred through shear from the matrix to the particles resulting low stress in the matrix. The stress transfer from the matrix to the nanoparticle was less for the nanocomposites without interphase resulting high stress in the matrix. Landis and McMeeking (1999) assume that the fibers carry the entire axial load, and the matrix material only transmits shear between the fibers. Based on these assumptions alone, it is generally accepted that these methods will be most accurate when the fiber volume fraction V_f and the fiber-to-matrix moduli ratio E_f/E_m are high. In the present case the elastic moduli of AA5154 matrix and AlN nano particle are, respectively, 70.3 GPa and 330 GPa.

Table 1: Mechanical properties of AA5154 matrix and AlN nanoparticles

Property	AA5154	AlN
Density, g/cc	2.66	3.26
Elastic modulus, GPa	70.3	330
Ultimate tensile strength, MPa	310	270
Poisson's ratio	0.33	0.24

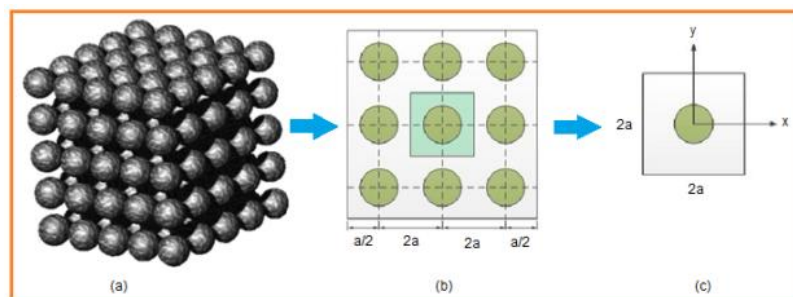


Figure 1: A square RVE containing a nanoparticle.

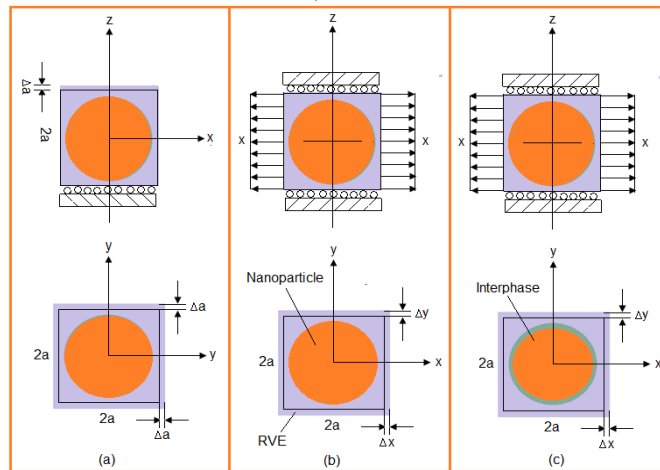


Figure 2: RVE models

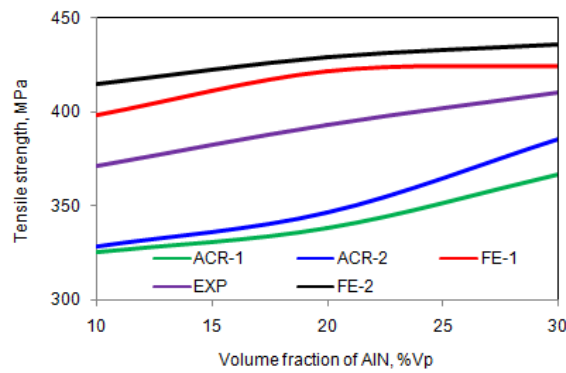


Figure 3: Effect of volume fraction on tensile strength along tensile load direction.

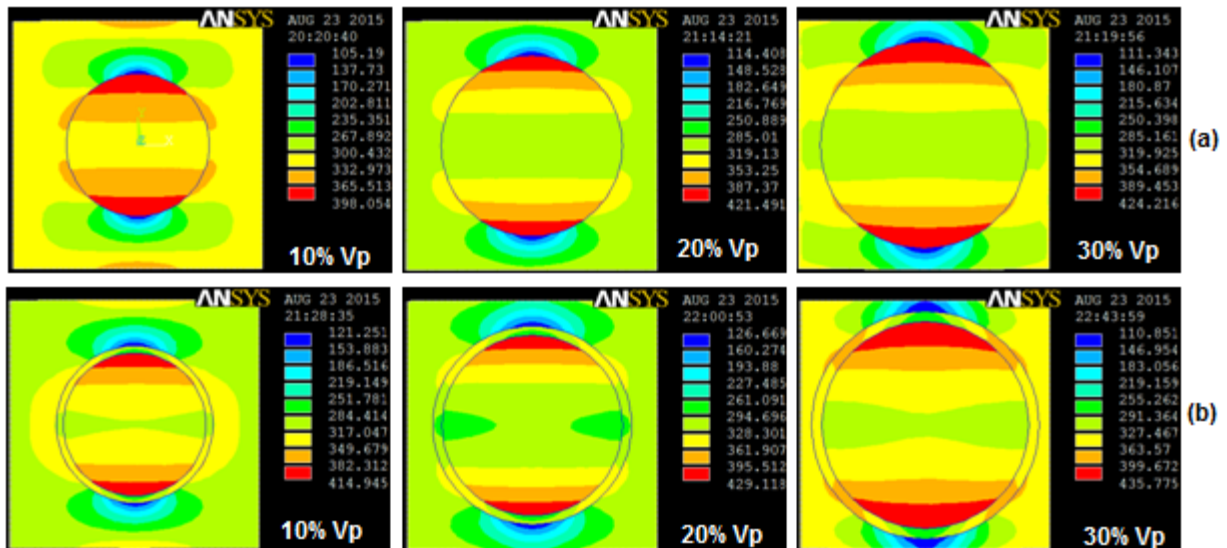


Figure 4: Tensile stresses (a) without interphase and (b) with interphase normal to load direction.

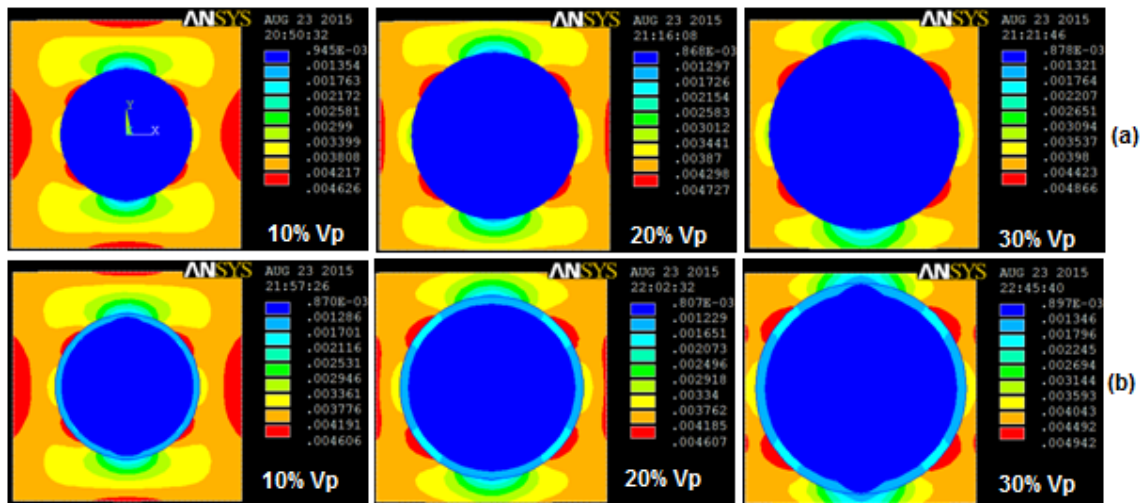


Figure 5: Elastic strain (a) without interphase, parallel, (b) with interphase, normal, (c) without interphase, parallel and (d) with interphase, normal to load direction.

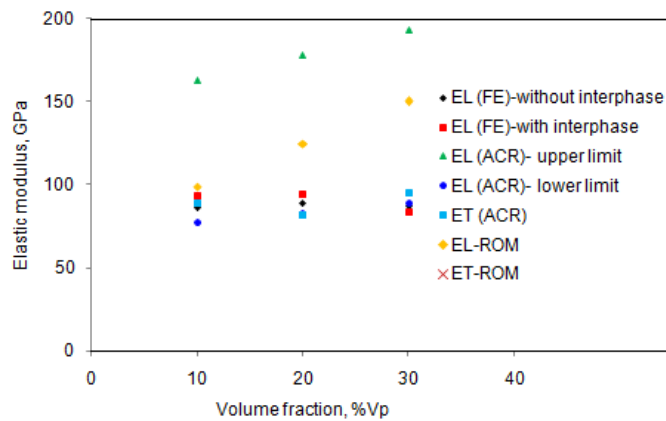


Figure 6: Elastic moduli of AA3105/AlN nano composite.

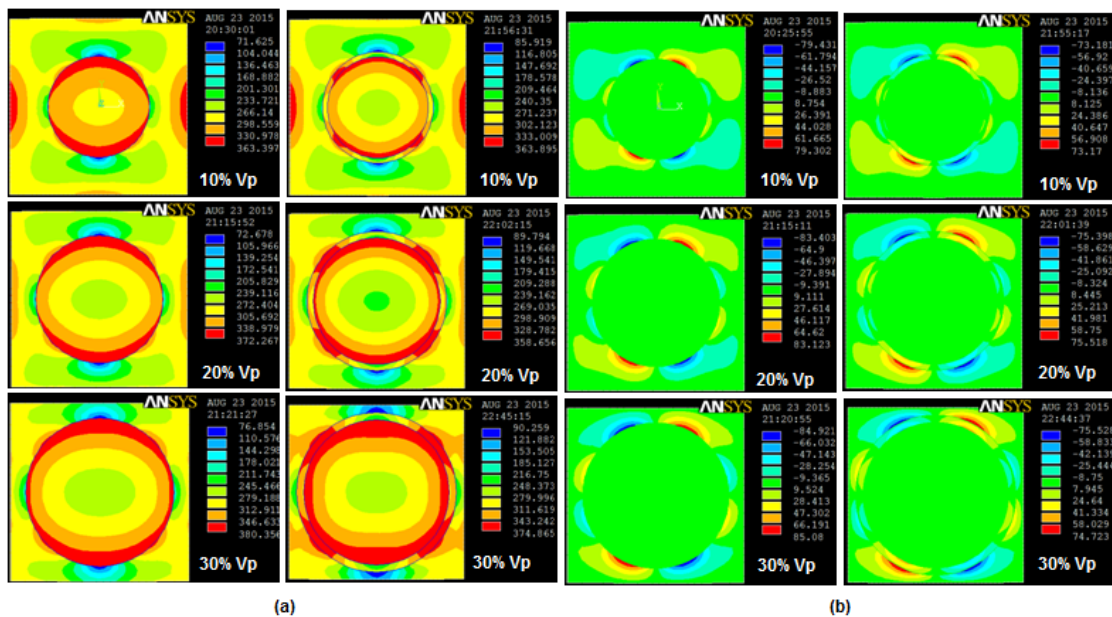


Figure 7: von Mises stress (a) and shear stress (b).

4. Conclusion

The RVE models give the trend of phenomenon happening in the nanocomposites. Without interphase and barely consideration of adhesive bonding, the tensile strength has been found to be 424.22 MPa for the nanocomposites consisting of 30% Aln nanoparticles. Due to interphase between the nanoparticle and the matrix, the tensile strength increases to 435.78 MPa. The tensile strengths obtained by author's model (with voids) are in good agreement with the experimental results. In the case of nanocomposites with interphase between the nanoparticle and the matrix, the stress is transferred through shear from the matrix to the particles. The transverse moduli of AlN/AA5154 nanocomposites have been found to be 23.87 GPa and 20.35 GPa, respectively, without and with interphase.

Acknowledgements

The author thanks the University Grants Commission (UGC), New Delhi for sanctioning this major project. The author also thanks the Central University, Hyderabad for providing the SEM images to complete this manuscript.

References

- Chennakesava Reddy A. (2004).** Analysis of the Relationship Between the Interface Structure and the Strength of Carbon-Aluminum Composites. NATCON-ME, Bangalore, India.
- Chennakesava Reddy, A. (2009).** Mechanical properties and fracture behavior of 6061/SiCp Metal Matrix Composites Fabricated by Low Pressure Die Casting Process. *J. Manuf. Technol. Res.* 1(3/4):273-286.
- Chennakesava R Alavala (2008).** Finite element methods: Basic concepts and applications," PHI Learning Pvt. Ltd, New Delhi.
- Chennakesava Reddy, A. and Essa Zitoun. (2009).** Matrix alloys for alumina particle reinforced metal matrix composites. *Indian Foundry J.* 55:12-16.
- Chennakesava Reddy, A and Essa Zitoun (2011).** Tensile properties and fracture behavior of 6061/Al₂O₃ metal matrix composites fabricated by low pressure die casting process. *Int. J. Mater. Sci.* 6(2):147-157.
- Chennakesava Reddy, A. (2015).** Cause and Catastrophe of Strengthening Mechanisms in 6061/Al₂O₃ Composites Prepared by Stir Casting Process and Validation Using FEA. *Int. J. Sci. Res.* 4:1272-1281.
- Davidson, A.M. and Regener, D. (2000).** A comparison of aluminium based metal matrix composites reinforced with coated and uncoated particulate silicon carbide. *Compo. Sci. Technol.* 60:865-869.
- Deng, X. and Chawla, N. (2006).** Modeling the effect of particle clustering on the mechanical behavior of SiC particle reinforced Al matrix composites. *J. Mater. Sci.* 41:5731-5734.
- Hill, R. (1963).** Elastic properties of reinforced solids: some theoretical principles. *J. Mech. Phy. Solids.* 11:357-372.
- Kotiveerachari, B. and Chennakesava Reddy, A. (1999).** Interfacial effect on the fracture mechanism in GFRP composites. CEMILAC Conference, Ministry of Defense, India.
- Landis, C.M. and McMeeking, R.M. (1999).** Stress concentrations in composites with interface sliding, matrix stiffness, and uneven fiber spacing using shear lag theory. *Int. J. Solids Struct.* 41:289-6313.
- Liu, Y.J. and Chen, X.L. (2003).** Evaluations of the effective material properties of carbon nanotube-based composites using a nanoscale representative volume element. *Mech. Mater.* 35:69-81.
- Reeves, A.J., Dunlop, H. and Clyne, T.W. (1992).** The effect of interfacial reaction layer thickness on fracture of titanium-SiC particulate composites. *Metall. Trans. A.* 23:977-988.
- Ren, S., Shen, X., Qu, X. and He, X. (2011).** Effect of Mg and Si on infiltration behavior of Al alloys pressureless infiltration into porous SiCp performs. *Int. J. Minerals, Metall. Mater.* 18:703-708.
- Sobczak, N., Ksiazek, M., Radziwill, W., Morgiel, J., Baliga, W. and Stobierski, L. (1997).** Effect of titanium on wettability and interfaces in the Al/ SiC system. in: *Proceedings of the International Conference High Temperature Capillarity, Cracow, Poland.*
- Zhengang Liuy, Guoyin Zu, Hongjie Luo, Yihan Liu and Guangchun Yao. (2010).** Influence of Mg Addition on Graphite Particle Distribution in the Al Matrix Composites. *J. Mater. Sci. Technol.* 26:244-pp.244-250.